AD-A142 418 SURFACE-ENHANCED RAMAN SCATTERING FOR REDOX-ACTIVE ADSORBATES: PENTAAMMIN.. (U) PURDUE UNIV LAFAYETTE IN DEPT OF CHEMISTRY S FARQUHARSON ET AL. APR 84 TR-29 1/1

UNCLASSIFIED N00014-79-C-0670 F/G 7/4 NL

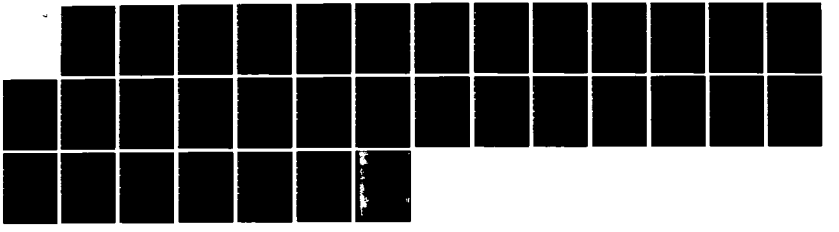

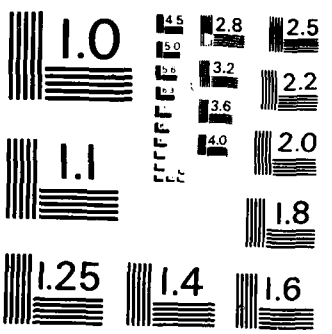

MICROCOPY RESOLUTION TEST CHART
NATIONAL BUREAU OF STANDARDS - 1963 - A

OFFICE OF NAVAL RESEARCH

Contract N00014-79-0670

TECHNICAL REPORT NO. 29

Surface-Enhanced Raman Scattering for Redox-Active Adsorbates: Pentaammineosmium(III)/(II) and Pentaammineruthenium(II) Containing Nitrogen Heterocycle Ligands

by

Stuart Farquharson, Kendall L. Guyer, Peter A. Lay,

Roy H. Magnuson and Michael J. Weaver

Prepared for Publication

in the

Journal of American Chemical Society

Department of Chemistry

Purdue University

West Lafayette, IN 47907

April 1984

SECURITY CLASSIFICATION OF THIS PAGE *(When Data Entered)*

REPORT DOCUMENTATION PAGE	READ INSTRUCTIONS BEFORE COMPLETING FORM
1. REPORT NUMBER: Technical Report. No. 29 — 2. GOVT ACCESSION NO.: AD-A142 418	3. RECIPIENT'S CATALOG NUMBER
4. TITLE *(and Subtitle)*: Surface-enhanced Raman Scattering for Redox-Active Adsorbates: Pentaammineosmium(III)/(II) and Pentaammineruthenium(II) Containing Nitrogen Heterocycle Ligands	5. TYPE OF REPORT & PERIOD COVERED: Technical Report No. 29 6. PERFORMING ORG. REPORT NUMBER
7. AUTHOR(s): Stuart Farquharson, Kendall L. Guyer, Peter A. Lay, Roy H. Magnuson, and Michael J. Weaver	8. CONTRACT OR GRANT NUMBER(s): N00014-79-0670
9. PERFORMING ORGANIZATION NAME AND ADDRESS: Department of Chemistry, Purdue University, West Lafayette, IN 47907	10. PROGRAM ELEMENT, PROJECT, TASK AREA & WORK UNIT NUMBERS
11. CONTROLLING OFFICE NAME AND ADDRESS: Office of Naval Research, Department of the Navy, Arlington, VA 22217	12. REPORT DATE: April 1984 13. NUMBER OF PAGES
14. MONITORING AGENCY NAME & ADDRESS*(if different from Controlling Office)*	15. SECURITY CLASS. *(of this report)*: Unclassified 15a. DECLASSIFICATION DOWNGRADING SCHEDULE

16. DISTRIBUTION STATEMENT *(of this Report)*

Approved for public release; distribution unlimited

17. DISTRIBUTION STATEMENT *(of the abstract entered in Block 20, if different from Report)*

18. SUPPLEMENTARY NOTES

19. KEY WORDS *(Continue on reverse side if necessary and identify by block number)*

SERS, silver-aqueous interface, rapid cyclic voltammetry, enhancement

20. ABSTRACT *(Continue on reverse side if necessary and identify by block number)*

Surface-Enhanced Raman Scattering (SERS) for pentaammineosmium(III) and pentaammineruthenium(II) containing pyridine (py), pyrazine (pz), or 4,4'-bipyridine (bpy) ligands adsorbed at the silver-aqueous interface has been examined as a function of electrode potential to explore vibrational changes associated with electron transfer involving simple adsorbates. SERS was observed for the pyridine complexes despite their lack of an unshared electron pair for surface binding, although more intense spectra were obtained for the pyrazine and bipyridine complexes which contain a more remote nitrogen lone pair. SER

DD FORM 1 JAN 73 1473 EDITION OF 1 NOV 65 IS OBSOLETE

SECURITY CLASSIFICATION OF THIS PAGE *(When Data Entered)*

vibrational bands for metal-ligand and internal ammine modes were observed in addition to those due to heterocycle ring modes. Marked shifts were observed in the frequency of several vibrational bands for adsorbed $Os(NH_3)_5py$ and $Os(NH_3)_5pz$ as the electrode potential was made more negative that are consistent with the reduction of Os(III) to Os(II). The potential-dependent concentrations of adsorbed Os(III) and Os(II) as determined using SERS are in good agreement with those obtained from rapid cyclic voltammetry. The bulk-phase Raman spectra exhibit resonance enhancement. Such electronic resonance also contributes to the overall signal enhancement seen in the SER spectra. The oxidation-state dependent signal enhancement seen for $Os(NH_2)_5pz$ indicates that its electronic properties are modified by adsorption.

SURFACE-ENHANCED RAMAN SCATTERING FOR REDOX-ACTIVE ADSORBATES: PENTAAMMINEOSMIUM(III)/(II) AND PENTAAMMINERUTHENIUM(II) CONTAINING NITROGEN HETEROCYCLE LIGANDS

Stuart Farquharson,[1a] Kendall L. Guyer,[1b] Peter A. Lay,[1c]
Roy H. Magnuson,[1c] and Michael J. Weaver[1a*]

Contribution from the Department of Chemistry, Purdue University,
West Lafayette, IN 47907 and
Department of Chemistry, Stanford University, Stanford, CA 94305

ABSTRACT

Surface-Enhanced Raman Scattering (SERS) for pentaammineosmium(III) and pentaammineruthenium(II) containing pyridine (py), pyrazine (pz), or 4,4'-bipyridine (bpy) ligands adsorbed at the silver-aqueous interface has been examined as a function of electrode potential to explore vibrational changes associated with electron transfer involving simple adsorbates. SERS was observed for the pyridine complexes despite their lack of an unshared electron pair for surface binding, although more intense spectra were obtained for the pyrazine and bipyridine complexes which contain a remote nitrogen lone pair. SER vibrational bands for metal-ligand and internal ammine modes were observed in addition to those due to heterocycle ring modes. Marked shifts were observed in the frequency of several vibrational bands for adsorbed $Os(NH_3)_5py$ and $Os(NH_3)_5pz$ as the electrode potential was made more negative that are consistent with the reduction of Os(III) to Os(II). The potential-dependent concentrations of adsorbed Os(III) and Os(II) as determined using SERS are in good agreement with those obtained from rapid cyclic voltammetry. The bulk-phase Raman spectra exhibit resonance enhancement, Such electronic resonance also contributes to the overall signal enhancement seen in the SER spectra. The oxidation-state dependent signal enhancement seen for $Os(NH_3)_5pz$ indicates that its electronic properties are modified by adsorption.

INTRODUCTION

The recent discovery of Surface-Enhanced Raman Scattering (SERS) for adsorbates at silver, copper, and gold surfaces has generated much experimental and theoretical activity aimed at understanding the underlying physical phenomena.[2] The SERS technique also holds promise as a major tool for investigating the detailed molecular properties of adsorbates in electrochemical environments, for which spectroscopic examination had previously been impractical.[2a,c] Although a variety of electrochemical adsorbates have now been demonstrated to yield SERS, surprisingly few attempts have been made to quantitatively relate the nature and intensity of SERS signals to the electrochemical properties of the system.

To this end, the Purdue group has been examining SERS of structurally simple adsorbates at silver-aqueous interfaces for which independent information can be obtained on the surface composition and structure.[3-5] In particular, we have demonstrated simple relationships between the intensity of SERS signals and the coverage for a number of simple anionic adsorbates as determined from corresponding capacitance-potential data.[3] Our overall objective is to utilize SERS not only to gain detailed information on structure and bonding for electrochemical adsorbates, but also to follow molecular transformations, especially electron-transfer reactions, at electrode surfaces.

For initial study we selected electrode reactions involving simple one-electron transfer for which both redox states are detectably adsorbed and structurally similar. Although suitable model systems are not abundant, a number of Os(III)/(II) and Ru(III)/(II) pentaammine couples exhibit several desirable features. In particular, $Os(NH_3)_5L^{III/II}$ and $Ru(NH_3)_5L^{III/II}$ are substitutionally inert in both oxidation states for a number of coordinated ligands, L, which are also capable of binding to metal surfaces. Suitable bridging ligands include simple inorganic

anions and organic ligands such as nitrogen heterocycles that contain an aromatic ring and/or a functional group expected to adsorb at silver. Suitably intense SER spectra were obtained for pentaammineruthenium(II) and pentaammineosmium(III) complexes containing pyridine (py) and pyrazine (pz), adsorbed at silver surfaces. Some spectra were also obtained for $Os^{III}(NH_3)_5bpy$ (bpy = 4,4'-bipyridine). Although the $Ru(NH_3)_5L^{III/II}$ couples have bulk-phase formal potentials, E_b^f, that are somewhat more positive (60 and 245 mV vs. sce for L = py and pz, respectively[7a]) than the potential region (ca. 0 to -1.0 V vs sce) typically available at silver-aqueous interfaces, the corresponding $Os(NH_3)_5L^{III/II}$ couples have values of E_b^f that lie within this region (E_b^f = -650, -240, and -465 mV vs sce for L = py, pz, and bpy, respectively[7b,c]). The latter adsorbates are therefore expected to be present in either the III or II oxidation state at silver, depending on the applied potential. Alteration of the osmium oxidation state is expected to yield significant changes in the vibrational properties of the heterocyclic ring as well as in the metal-nitrogen modes since the added electron will be extensively delocalized via π-bonding. Such adsorbed redox couples having nitrogen heterocycle bridging groups constitute heterogeneous analogs of the much-studied intramolecular redox systems in homogeneous solution.[8] An additional reason for selecting these systems is that nitrogen heterocycles have received extensive scrutiny as model adsorbates for SERS at silver.[2]

We present here SER spectra for these osmium and ruthenium complexes as a function of electrode potential. These are compared with corresponding vibrational spectra for the bulk-phase metal complexes in both III and II forms, along with electrochemical data for the adsorbed Os(III)/(II) couples, in order to explore the ability of SERS to detect redox transformations at metal surfaces. The potential-dependent surface concentrations of the Os(III) and Os(II) adsorbates

as determined using SERS are compared with corresponding data obtained by conventional electrochemical means. A preliminary communication describing SERS of adsorbed $Os(NH_3)_5py^{III/II}$ has already appeared.[5a] A complete compilation of the various vibrational bands, along with a detailed discussion of the vibrational mode assignments, is given elsewhere.[9]

EXPERIMENTAL

The various pentaammineruthenium(II) and pentammineosmium(III) complexes with pyridine, pyrazine and 4,4'-bipyridine ligands were prepared as halide or trifluoromethanesulfonate salts essentially as detailed elsewhere.[10a,b] Both SERS and electrochemical studies employed 0.05-1 mM aqueous solutions in either 0.1 M NaCl or NaBr, which also contained 0.1 M HCl in the case of the pyridine complexes to suppress base-catalyzed disproportionation.[11] Ammine deuteration was performed by dissolving the complexes in neutral D_2O followed by acification after ca 5 min.

Raman excitation was obtained using either a Spectra Physics Model 165 Kr^+ laser (647.1 nm) or Ar^+ laser (514.5 nm). Both a scanning double monochromator (either a Jarrell-Ash Model 25/100 or a SPEX 1403) and, later, a triple spectrograph-optical multichannel analyzer (OMA) arrangement (SPEX 1877-PAR OMA 2) were utilized to obtain Raman spectra. Further details of the Raman and infrared experimental procedures are given in ref. 9. The silver electrode was of rotating disk construction, having an exposed face of diameter 0.4 cm, encased by a Teflon shroud. It was mechanically polished successively with 1.0μ and 0.3μ alumina immediately before immersion in the cell. It was then electrochemically roughened in order to optimise the SERS intensities by means of an oxidation-reduction cycle (ORC) in the conventional manner,[2a] using a PAR 173 potentiostat with a PAR 179 digital coulometer. A typical ORC entailed stepping the potential from -150 to +250 mV, and return after the passage of 40 mC cm^{-2} of anodic charge.

(This roughening procedure increases the actual silver surface area only ca. twofold.[3b]) The PAR 173 potentiostat was also used along with a PAR 175 potential programmer and a Houston 2000 X-Y recorder or a Nicolet 2090-1 digital oscilloscope to obtain cyclic voltammograms for both bulk solution and surface-bound redox couples. All experiments were conducted at 23 ± 1°C and all electrode potentials are quoted with respect to the saturated calomel electrode (sce).

RESULTS

Electrochemistry of Adsorbed Os(III)/(II) Couples

Cathodic-anodic cyclic voltammetry of the $Os(NH_3)_5py^{III/II}$ couple at silver as well as at a hanging mercury electrode yielded a reversible wave with E_b^f = -650 mV in 0.1 M HCl. These voltammograms were obtained under conventional conditions (sweep rates ca. 100-500 mV sec^{-1}; reactant concentration ca. 1 mM) for which the contribution from any initially adsorbed reactant is negligible. However, if the oxidized and reduced forms are sufficiently strongly adsorbed, the formal potential for the adsorbed redox couple can also be obtained using cyclic voltammetry. This entails using sufficiently rapid sweep rates ($\gtrsim$ 20 V sec^{-1}) and small bulk reactant concentrations ($\lesssim$ 0.1 mM) so that the faradaic current arises almost entirely from reaction of the initially adsorbed, rather than the diffusing, reactant. Figure 1A shows such a cyclic voltammogram for adsorbed $Os(NH_3)_5py^{III/II}$ at a roughened silver electrode in 0.1 M NaCl + 0.1 M HCl; the sweep rate was 200 V sec^{-1} and the bulk concentration, C_b, of $Os(NH_3)_5py^{3+}$ equalled 0.05 mM. The almost symmetrical shape and near coincidence of the cathodic and anodic peak potentials, together with the observed linear dependence of the peak current upon sweep rate, indicate that the waves arise from initially adsorbed reactant. (The small separation between the cathodic and anodic peaks is probably due to uncompensated cell resistance.)

The formal potential for the adsorbed $Os(NH_3)_5py^{III/II}$ couple, E_a^f, is determined as 670 ± 5 mV from the position of the peak potentials. Reactant surface

concentrations of 3 to 4 x 10^{-11} mole cm^{-2} (for C_b = 0.05 m$\underline{M}$) were typically obtained from the faradaic charge contained under the voltammetric waves. The full width at half-peak height, $\Delta E_{p,\frac{1}{2}}$ = 95 mV, is close to the value, 91 mV, expected for a reversible adsorbed couple obeying the Langmuir isotherm.[12] Comparable results were also obtained for adsorbed $Os(NH_3)_5py^{III/II}$ in electrolytes containing 0.1 $\underline{M}$ NaBr (*vide infra*), with E_a^f = -700 mV and $\Delta E_{p,\frac{1}{2}}$ = 125 mV.

Similar measurements for solutions of $Os(NH_3)_5pz^{3+}$ in 0.1 $\underline{M}$ NaCl (pH 9) yielded somewhat less well-defined surface voltammograms, although a peak for adsorbed $Os(NH_3)_5pz^{III/II}$ was detected for C_b = 0.1 m$\underline{M}$, corresponding to E_a^f = -335 mV (Fig. 2A). More pronounced surface voltammograms were obtained for $Os(NH_3)_5bpy^{III/II}$, with E_a^f = -490 mV in 0.1 $\underline{M}$ NaCl (C_b = 50 μM). Although such voltammograms might conceivably be due to nonfaradaic (i.e. capacitive) rather than faradaic current, this is unlikely since no such peaks were detected in the absence of the adsorbate. The values of E_a^f in each case are not far from the values of E_b^f noted above for the corresponding bulk redox couples. The corresponding three ruthenium complexes yielded no detectable surface-bound redox couples within the available potential range (0 to -1.0 V), as expected in view of the positive bulk formal potentials for these systems (vide supra).

SERS of $Os(NH_3)_5py$ and $Ru(NH_3)_5py$

Following an ORC at a roughened silver electrode in electrolytes containing either 0.1 $\underline{M}$ NaBr and 0.1 $\underline{M}$ NaCl, SER spectra were obtained for $Os(NH_3)_5py$ and $Ru(NH_3)_5py$ over the potential range -150 and -750 mV. (Note that metal oxidation states will be omitted when referring to the adsorbed complexes except for conditions where they are clearly known.) Representative spectra of $Os(NH_3)_5py$ and $Ru(NH_3)_5py$ for several key frequency regions are shown in Figs. 3 and 4, respectively. Tabulations of the most important vibrational modes seen for these two systems at a representative pair of electrode potentials are given in Tables

I and II. The pyridine ring modes are assigned Wilson numbers in accordance with established procedure.[13] These tables also contain summaries of the corresponding normal Raman and IR vibrational bands for the bulk-phase complexes in both III and II oxidation states. Table II additionally contains SERS data for pyridine obtained under similar conditions; the observed peak frequencies agree closely with previous detailed reports.[14,15] More complete tabulations of the Raman and IR spectra for these and the other complexes considered here, along with a more detailed discussion of the vibrational assignments, are given elsewhere.[9] The SER spectra were generally stable for at least 30-60 mins using both 514.5 or 647.1 nm irradiation. However, significant intensity losses typically occurred at more negative potentials when using chloride rather than bromide electrolytes. The SER spectra could nonetheless be almost entirely regenerated by repolishing the electrode followed by another ORC.

The various mode assignments listed were made on the basis of group symmetry considerations, and by comparison of the relative frequencies and intensities with those for the Raman and IR spectra of uncoordinated pyridine [14-16] and a number of metal pyridine,[17] pyrazine,[18] and ammine[19] complexes for which detailed assignments are available. Although the normal Raman spectra of the bulk-phase complexes are too weak to detect all but the most prominent bands, the corresponding SERS spectra were sufficiently intense to exhibit these and most of the modes seen in the bulk-phase IR spectra.

A further aid to vibrational assignments for $Os(NH_3)_5py$ was provided by examining the frequency shifts in the SER spectra brought about by separate deuteration of the pyridine ring or ammine hydrogens. The resulting peak frequencies are also included in Table I. SER spectra were also obtained for pyridine-deuterated $Ru(NH_3)_5py$; the peak frequencies obtained for this system are shown in parentheses in Table II. These frequency shifts enable a distinction to

made between vibrational modes associated chiefly with the ammine and pyridine ligands.[9] For example, the SERS peak at 468 cm^{-1} (-750 mV) shifts to a markedly lower frequency (436 cm^{-1}) upon ammine deuteration than that resulting from pyridine deuteration (461 cm^{-1}). This supports the assignment of this band to an osmium-ammine stretching mode. Indeed, the frequency ratio for the hydrogen to deuterium ammines (0.93), is close to the corresponding ratio (0.92) observed for ammine deuteration in $Ru(NH_3)_6^{3+}$.[19a] The strong bands seen at 267 cm^{-1} for $Os(NH_3)_5py$ and at about 300 cm^{-1} for $Ru(NH_3)_5py$ are assigned to a metal-pyridine stretching mode on the basis of the very similar frequencies observed for this mode in a number of other transition-metal pyridine complexes.[17] The slight frequency decreases seen for this band upon ammine deuteration (Table I) are consistent with coupling between the metal-pyridine and metal-ammine vibrations.

The frequency shifts seen in the SER spectra for $Os(NH_3)_5py^{III/II}$ and $Ru^{II}(NH_3)_5py$ upon deuterating the pyridine ring are uniformly in good agreement with corresponding shifts seen both for bulk pyridine and several metal pyridine complexes.[19,20] Although most of the bands in the frequency region above ca. 600 cm^{-1} are associated with pyridine ring modes, there is also evidence for the appearance of internal ammine modes in the SER spectra. Thus the strong NH_3 bending mode at 1620 cm^{-1} for $Os(NH_3)_5py$ (-150 mV) shifts to 1170 cm^{-1} upon ammine deuteration, similar to that observed for several metal ammine complexes.[18c]

Peaks at 240 cm^{-1} and 180 cm^{-1} were also observed in chloride and bromide electrolytes, respectively. Since very similar bands are also observed in pure halide electrolytes[3c,20] and the pyridine complexes lack an electron lone pair for surface binding, they are attributed to surface-halide stretching modes. All the absorbate vibrational bands occurred at essentially identical frequencies in chloride- and bromide-containing electrolytes. However, the latter medium was

employed for most measurements since it yielded more stable SER spectra, especially at more negative potentials.

The SER spectra for $Os(NH_3)_5py$ and $Ru(NH_3)_5py$ exhibit two significant differences as the potential is made progressively more negative. Firstly, the signal intensity for the latter system decreases to a markedly greater extent than for the former. Secondly, several peaks in the $Os(NH_3)_5py$ spectrum disappear, being replaced by peaks at lower frequencies. In particular, the osmium-ammine stretch at 494 cm^{-1} and the symmetric ring-breathing mode at 1020 cm^{-1}, both present within the potential region ca. -100 to -600 mV, are replaced at more negative potentials by peaks at 468 and 992 cm^{-1}, respectively (Fig. 3). A peak at 267 cm^{-1}, tentatively assigned to a metal-pyridine mode,[9] also appears at more negative potentials (Fig. 3).[21] Such a frequency decrease for the metal-ammine mode is consistent with a reduction of Os(III) to Os(II) (vide infra).[19] The frequency shift for the symmetric ring-breathing mode (Wilson mode 1) corresponds closely to the frequency difference seen in the IR spectra of $Os^{III}(NH_3)_5py$ and $Os^{II}(NH_3)_5py$ (Table I). A sufficiently pure sample of $Os^{II}(NH_3)_5py$ could not be obtained to allow the corresponding frequency shifts for the other modes to be determined. However, a comparison with the corresponding spectral differences between bulk-phase $Ru^{III}(NH_3)_5py$ and $Ru^{II}(NH_3)_5py$ (Table II) indicates that the frequency shifts seen for other modes in the SER spectra of $Os(NH_3)_5py$ beyond ca. -600 mV are also consistent with a decrease in metal oxidation state. Other SERS bands for $Os^{III}(NH_3)_5py$ also exhibit significant frequency changes upon reduction to Os(II). In particular, the asymmetric ring breathing mode shifts from 1076 to 1054 cm^{-1}, and the symmetric N-H bending mode from 1354 to 1 cm^{-1} (Table I).

The relative peak intensities of the 1020 and 992 cm^{-1} SERS vibrational bands of $Os(NH_3)_5py$, I^P_{III} and I^P_{II}, respectively, are plotted (dashed lines) as a function of electrode potential in Fig. 1B. (The potential-dependent spectra used

to construct Fig. 1B were obtained using the optical multichannel analyzer to minimize errors arising from the temporal decay of the Raman signals.[5c] The intensities are normalized to the values seen at the potentials, ca. -450 mV and -800 mV, for the 1020 cm^{-1} and 992 cm^{-1} modes, respectively. These potentials span the region within which one band is replaced entirely by the other. For comparison, corresponding plots of the relative surface concentrations of $Os(NH_3)_5py^{III}$ and $Os(NH_3)_5py^{II}$, Γ_{III} and Γ_{II}, respectively, are shown as solid curves in Fig. 1B. These were obtained by integrating the cyclic voltammogram in Fig. 1A to yield faradaic charge-potential (q_f-E) plots, from which the normalized Γ-E plots were obtained directly since $q_f \propto \Gamma$. (Note that Γ_{III} and Γ_{II} are related by $\Gamma_{III} = 1 - \Gamma_{II}$.) Formal potentials for the adsorbed Os(III)/(II) couple may conveniently be obtained from the intersection of the corresponding Os(III)-E and Os(II)-E curves. That determined from SERS, $E^f_{SER} = -670 \pm 10$ mV, is identical to the cyclic voltammetric value, E^f_a (vide supra). (This supplants the earlier reported value[5a] of -630 mV, obtained using a scanning spectrometer.) Corresponding SERS data gathered in bromide electrolytes yielded similar results, with $E^f_{SERS} \approx E^f_a$.

SERS of $Os(NH_3)_5pz$ and $Ru(NH_3)_5pz$; Relative Raman Intensities

SER spectra were recorded for solutions containing ca. 0.1 mM $Os(NH_3)_5pz^{3+}$ and $Ru(NH_3)_5pz^{2+}$ in 0.1 M NaCl or 0.1 M NaBr as a function of electrode potential under similar conditions to those employed for the pyridine complexes. Representative spectra for some key frequency regions are shown for $Os(NH_3)_5pz$ and $Ru(NH_3)_5pz$ in Figs. 5 and 6, respectively. The various vibrational bands observed for these systems are summarized in Tables III and IV, together with the corresponding bands obtained for SERS of pyrazine obtained under similar conditions and normal Raman and IR spectra of the bulk complexes in III and II oxidation states. The vibrational assignments given in these Tables are based partly on comparisons with those given previously for pyrazine[13,15] and for bulk-phase metal pyrazine complexes.[18]

Several features of these SER spectra are worthy of particular comment. Firstly, most vibrational bands associated with ring modes in both the $Os(NH_3)_5pz$ and $Ru(NH_3)_5pz$ SER spectra are 10- to 50-fold more intense than in the SER spectra for the corresponding pyridine complexes. Secondly, in contrast to the behavior of the corresponding pyridine complexes, most bands in the $Os(NH_3)_5pz$ spectra become more intense as the potential is made more negative. The intensity of the $Ru(NH_3)_5pz$ spectra is only mildly potential dependent (Figs. 5 and 6). Thirdly, the SER spectral features seen in the 150-400 cm^{-1} region for both $Os(NH_3)_5pz$ and $Ru(NH_3)_5pz$ differ markedly from those seen for either the corresponding bulk spectra or the SER spectra for the pyridine complexes. Thus $Os(NH_3)_5pz$ exhibits intense peaks at 304 and 345 cm^{-1} (Fig. 5) whereas $Ru(NH_3)_5pz$ yields a single broad peak around 300-325 cm^{-1}, the frequency depending on the potential (Fig. 6).

The potential-dependent SER spectra for $Os(NH_3)_5pz$ (Fig. 5) are in some respects similar to those for $Os(NH_3)_5py$. Thus bands appear at both 1020 and 985 cm^{-1}, which as for the pyridine analog can be assigned to the symmetric ring breathing modes in Os(III) and Os(II), respectively, on the basis of the frequencies in the bulk-phase spectra (Table III). However, unlike $Os(NH_3)_5py$ there is no straightforward potential-dependent substitution of Os(III) by the corresponding Os(II) bands. Instead, altering the potential to more negative values in the vicinity of E_a^f (~335 mV, vide supra) yields a dramatic increase in the intensity of several $Os(NH_3)_5pz$ bands associated with Os(II) (particularly those at 673, 985, and 1067 cm^{-1}, Fig. 5). This occurs without a sizable decrease in some bands expected to be associated with Os(III), especially that at 1020 cm^{-1}. Nevertheless, these results may be rationalized by referring to the corresponding solution Raman spectra for 2.5 mM $Os(NH_3)_5pz^{3+}$ and $Os(NH_3)_5pz^{2+}$, a segment of which is also shown in Fig. 5. The normal Raman Os(II) bands are substantially more intense than those

for Os(III). In particular, mode 12 for Os(II) (1067 cm^{-1}) increases dramatically relative to that for the Os(III) form (1090 cm^{-1}).

With this in mind, a plot of the potential-dependent peak intensities of the 1093 and 1067 cm^{-1} bands in the $Os(NH_3)_5pz$ SER spectra was prepared (cf Fig. 1B); this is shown in Fig. 2B. As in Fig. 1B, the SERS data are compared with the Os(III)/(II) surface redox behavior determined from rapid cyclic voltammetry (Fig. 2A). Although the latter band is considerably more intense, once normalized to their values at potentials spanning the potential-dependent region (ca. -200 to -450 mV) reasonable correspondence between the Os(III)/(II) redox behavior sensed by SERS and conventional electrochemistry is again obtained. Thus the formal potential determined from SERS, E^f_{SER} = -310 ± 10 mV, is close to the voltammetric value, E^f_a = -335 mV (vide supra).

The survival of several bands at first sight due to $Os(NH_3)_5pz^{3+}$, especially those at 1020, 702, and 345 cm^{-1} (Fig. 5) even at potentials negative of this region is nevertheless puzzling. The band at 1020 cm^{-1}, at least, may be ascribed to adsorbed pyrazine, presumably present as an impurity.

The relative Raman scattering efficiencies for the complexes as well as for uncoordinated pyridine and pyrazine were determined both in aqueous solution and at the electrode surface. The latter utilized coverage data determined for the complexes as above, and for the free ligands from capacitance-potential measurements.[22] Although detailed data will be given elsewhere,[23] some results pertinent to the present study are now summarized. The internal heterocyclic modes in the solution-phase Raman spectra of the pyridine and pyrazine complexes were substantially (up to 10^3 fold) more intense than for the free ligands using 647 nm and especially 514.5 nm irradiation. This is indicative of electronic resonance enhancement, as might be expected in view of the proximity of the irradiation wavelengths to intense electronic adsorption bands for these complexes.[7c,10] Comparably larger intensities

were typically also seen in the SER spectra of the complexes relative to those for the absorbed ligands. Consequently, the surface enhancement factors (SEF) for these systems, i.e. the Raman scattering efficiency of the adsorbed relative to the corresponding bulk-phase species, were not greatly different, lying in the range ca. 1-10 x 10^6 (cf ref 2a). Nonetheless, some significant variations in SEF were observed. Especially large SEF were determined for $Os(NH_3)_5pz$, which were somewhat dependent on the laser excitation wavelength. Thus for mode 12 of $Os(NH_3)_5pz^{2+}$ (1067 cm^{-1}): at 514.5 nm, SEF ≈ 2.5 x 10^7, whereas at 647 nm, SEF ≈ 7.5 x 10^8.[23]

SERS of $Os(NH_3)_5$ bpy

Although the vibrational spectra of bipyridine complexes are rather more complicated than for single-ring heterocycles, the appearance of a well-defined adsorbed $Os(NH_3)_5bpy^{III/II}$ couple from cyclic voltammetry (vide supra) prompted us to examine SERS of $Os(NH_3)_5bpy$ as a function of electrode potential. A tabulation of the SER spectral bands along with vibrational assignments is given in ref. 9. Although alteration of the electrode potential to values negative of the formal potential for the adsorbed Os(III)/(II) couple (-490 mV, vide supra) yielded little change for most vibrational modes, the symmetric ring breathing mode at 1005 cm^{-1} decreased in intensity and a new band at 996 cm^{-1} appeared. By analogy with the results for the $Os(NH_3)_5py^{III/II}$ couple noted above, this may be associated with the formation of Os(II) from Os(III). However, this conclusion is tempered by the greater uncertainty in assigning such bands in view of the relative complicated structure of the adsorbate.

DISCUSSION

Since the silver electrode is composed of an array of surface sites having subtly different structural properties, given that only a minority of these sites may contribute predominantly to SERS [2] it is of central interest to compare the energetics of such "Raman-active" sites as measured by the potential-dependent Raman intensities with that for the overall surface as obtained from conventional electrochemistry.[3] The remarkable similarity in the potential dependence of the relative surface concentrations of $Os^{III}(NH_3)_5py$ and $Os^{II}(NH_3)_5py$, Γ_{III} and Γ_{II}, with the corresponding relative intensities of the symmetric ring modes, I^P_{III} and I^P_{II} (Fig. 1B), so that $E^f_a \approx E^f_{SER}$, indicate that the redox properties of the surface sites that are responsible for the observed Raman signals do not differ significantly from those for the sites occupied by the majority of the adsorbate. The same conclusion applies to the $Os(NH_3)_5pz^{III/II}$ couple (Fig. 2B), albeit with less certainty given the less straightforward nature of the Os(III)/(II) SERS behavior for this system.

As noted previously,[5a] the observation of SERS for the pyridine complexes is of significance in itself since no unshared electron pairs are available on the pyridine or ammine ligands with which to form an adsorbate-surface bond. Such bonding is commonly considered to be a desirable or even required feature for SERS.[2e] However, N-methylpyridinium has been shown to yield SERS at silver in the presence of adsorbed iodide,[24] and SERS have also been observed for $Ru^{III}(2,2'\text{-bipyridine})_3$ and related complexes.[25] Most strikingly, we have recently demonstrated that SERS can be obtained for transition-metal hexaammine cations at silver in the presence of adsorbed halide, even though such species clearly cannot interact specifically with the electrode surface.[5b] One such electroactive system, $Ru(NH_3)_6^{3+/2+}$, also yields a value of E^f_{SER} almost identical to that of E^f_a, measured as here by means of

rapid cyclic voltammetry.[5b] In common with the present adsorbed $Os(NH_3)_5py^{3+/2+}$ and $Os(NH_3)_5pz^{3+/2+}$ couples, $Ru(NH_3)_6^{3+/2+}$ exhibits a value of E_a^f that is somewhat (20-100 mV) more negative of that for the solution-phase couple, E_b^f, in both chloride and bromide media. This shift is consistent with the expected double-layer potentials at the adsorption site, ϕ_R, generated by the extensive halide adsorption occurring at silver in this potential region (-200 to -700 mV).[3b] Thus on the basis of simple electrostatics, it is expected that $E_a^f = E_b^f + \phi_R$. Electrostatic double-layer attraction, clearly all-important for $Ru(NH_3)_6^{3+/2+}$, therefore appears also to be a crucial factor in generating the high interfacial concentrations (i.e. strong adsorption) seen for the present Os(III)/(II) couples in chloride or bromide media.

The possible surface orientations are restricted for the adsorbed pyridine complexes; inspection of molecular models shows that the ammine ligands will prevent the pyridine ring from lying flat on the electrode surface. These complexes may adsorb with the ring on edge,[26] oriented so to enable osmium or ruthenium to ion pair with the coadsorbed bromide or chloride anions. Indeed, the halide ions play an important role in stabilizing the SERS signals. This is evidenced by the decreases in SERS intensity, especially for $Ru^{II}(NH_3)_5py$, brought about by altering the potential to more negative values where the halide coverage decreases (Fig. 3),[3b,c] as indicated by the disappearance of the surface-halide stretching bands. Also worthy of comment is the appearance of SERS bands associated with metal-ammine and internal ammine modes in addition to metal-pyridine and internal pyridine modes (Tables I, II), even though the coupling between the ammine ligands and the electrode surface must be extremely weak (cf ref. 5b). Indeed, the intensities of the internal ammine modes relative to the nitrogen heterocycle modes are not substantially different in the SER and normal Raman spectra. All these findings clearly indicate that strong adsorbate-surface interactions are not a prerequisite for the observation of intense SERS.

A previous comparison of the bulk vibrational spectra of liquid pyridine with a number of divalent metal pyridine complexes has shown that the frequency of a number of pyridine ring modes, especially modes 6a (605 cm^{-1}), 1 (990 cm^{-1}), and 8a (1590 cm^{-1}), increase significantly upon coordination.[17d] These shifts can be ascribed in part to coupling with low frequency metal-pyridine vibrations.[17d] Similarly, the frequencies of most pyridine modes in the SER spectra of $Os^{III}(NH_3)_5py$, $Os^{II}(NH_3)_5py$, and $Ru^{II}(NH_3)_5py$ are close to, but significantly higher, than those for the corresponding bands in the SER spectra for free pyridine; a few modes, most notably the A_1 δ_{ring} mode (6a), exhibit 20-30 cm^{-1} higher frequencies in the metal complexes (Tables I, II). The close similarities in the frequencies of all modes in the SER spectra of these complexes with those in the corresponding bulk-phase spectra (Tables I, II) indicates that the silver surface exerts only a very minor perturbation on the bonding within these complexes.

The notably (10-30 cm^{-1}) lower frequencies of several metal-ligand and pyridine ring modes for $Os^{II}(NH_3)_5py$ compared with $Os^{III}(NH_3)_5py$ (Table I) are consistent with the high degree of metal to ligand back bonding expected for Os(II), yielding an increase of π electron density on the pyridine ring for $Os^{II}(NH_3)_5py$ compared to $Os^{III}(NH_3)_5py$. Interestingly, the frequency of the symmetric ring breathing mode for $Os^{II}(NH_3)_5py$ (992 cm^{-1}) is noticably lower than for $Ru^{II}(NH_3)_5py$ (1012 cm^{-1}). This mode is known to be especially sensitive to the pyridine environment.[27] This lower value of ν_{ring} for $Os^{II}(NH_3)_5py$ is consistent with the more extensive metal to ligand back bonding expected for Os(II) than for Ru(II),[28] and suggests that the force constant of the ring mode is decreased as a result of a greater nonbonding electron density.

The comparison between the SER spectra of the pyrazine and pyridine complexes is interesting since, unlike the latter, surface binding for the former complexes can occur via the remote pyrazine nitrogen. By analogy with the known influence of

coordination at the remote nitrogen upon the redox behavior of $Os(NH_3)_5pz^{III/II}$,[10b,c] surface attachment via this nitrogen might be expected to yield large (+ 200 mV) positive shifts in E_a^f resulting from stabilization of the Os(II) state. However, as noted above both the SERS and electrochemical data for $Os(NH_3)_5pz$ (Figs. 2,5) yield a formal potential, E_a^f ~ -320 mV is distinctly negative of that for the bulk couple, -240 mV. It is conceivable that a portion of the Os(II) adsorbate is sufficiently stabilized with respect to electrooxidation that it is effectively electroinactive at silver; however this is inconsistent with the loss of the Os(II) SER signals positive of ca. -300 mV. This therefore suggests that nitrogen surface coordination of $Os(NH_3)_5pz$ does not exert a major influence upon the redox behavior.

Nevertheless, some spectral features for the pyrazine complexes suggest that adsorbate-surface electronic coupling plays a more significant role than for the pyridine complexes. The appearance of especially intense bands around 300 cm^{-1} in the SER spectra of both $Os(NH_3)_5pz$ and $Ru(NH_3)_5pz$, attributed to metal-pyrazine stretching modes,[9] is of interest in this regard. The breadth of the $Ru(NH_3)_5pz$ band together with its potential dependence (Figure 6) suggests that it is composed of more than one vibrational mode; indeed, two distinct bands are seen for $Os(NH_3)_5pz$ (Fig. 5). These bands may well correspond to metal-pyrazine vibrations at different surface sites.

The especially large SEF seen for adsorbed $Os(NH_3)_5pz^{2+}$ suggests that significant modifications in the electronic properties are brought about by adsorption. Coordination of the pyrazine nitrogen to the metal surface might be expected to shift the prominent adsorption band, centered at 460 nm,[7c] to longer wavelengths by analogy with the effect of bulk-phase coordination.[10b,c] Such a shift

should further enhance the SER intensities, as observed, if a conventional electronic resonance effect is operative since the 514.5 and 647 nm laser irradiation lies within the long wavelength "tail" of the absorption band.

It is also worth noting here that the similarities seen in the degree of resonance enhancement for the bulk-phase and adsorbed pyridine and pyrazine complexes indicate that this "conventional resonance" effect simply forms a additional independent factor contributing to the overall SERS effect. This provides an argument against the currently popular notion[2e] that a major portion of the observed SERS effect commonly arises from "surface resonance" associated with adsorbate-metal charge-transfer excitations. Such a mechanism is inconsistent with the present finding that the additional signal enhancement, presumably due to "isolated molecule resonance", occurs at the surface to a comparable or greater extent than in bulk solution.

The difference in the potential dependencies of the overall SERS intensities for the pyridine and pyrazine complexes is also suggestive of nitrogen surface binding for the latter. As noted above, the appearance of SERS for the former adsorbates appears to require strong halide coadsorption. In contrast, SERS for the pyrazine complexes persists even at the most negative potentials (ca. -750 mV) where halide coadsorption is relatively weak. Presumably the nitrogen-bound pyrazine complexes can both create and stabilize "Raman-active" sites, whereas the surface sites responsible for SERS of pyridine complexes are both created and stabilized by surrounding halide anions.

The near-zero separation of the cathodic and anodic peak potentials for the adsorbed $Os(NH_3)_5py^{III/II}$ redox couple (Fig. 1A) indicate that the heterogeneous electron-transfer reaction is rapid on the electrochemical time scale ($\geq 10^{-3}$ sec). However, the presence of distinct vibrational modes associated with Os(III) and

Os(II) indicate that it is a valence-trapped (class II) system[29] on the vibrational time scale. This is expected in view of the relatively weak coupling between the oxmium redox center and the metal surface for this system. The SERS of $Os(NH_3)_5pz^{III/II}$ also shows hallmarks of class II behavior [cf. mixed-valence diruthenium complexes[30]].

CONCLUDING REMARKS

The foregoing demonstrates that SERS can provide a valuable tool for examining sequential redox states for adsorbed coordination compounds at metal surfaces. Particularly encouraging is the remarkably close correspondence between the potential-dependent redox equilibria for adsorbed transition-metal couples as sensed by SERS and that obtained from conventional electrochemistry, and the simple rationalization of the adsorption-induced changes in the redox equilibria in terms of electrostatic double-layer effects. It also suggests that SERS can usefully be employed to unravel redox pathways for more complex, electrochemical reactions involving adsorbed species where the identification of the intermediates and products can be fraught with difficulties.

In view of the intensity and richness of the SER spectra, the technique shows promise as a means of obtaining hitherto unavailable vibrational information for coordination compounds that can be electrostatically or chemically bound to silver electrodes. This includes oxidation states, such as Os(III), that are difficult to obtain in pure form in bulk media due to their chemical reactivity. Such information for sequential oxidation states is required in order to understand redox reactivity in terms of the molecular structural changes accompanying electron transfer. This approach also enables information to be gained for the first time on the molecular details associated with heterogeneous electron-transfer processes. Measurements of the dynamic as well as equilibrium properties of transition-metal adsorbates obtained using time-resolved SERS combined with conventional electrochemistry are underway in our laboratory.

ACKNOWLEDGMENTS

The electrochemical measurements were performed by Joseph Hupp. We thank George Leroi for the use of a Raman spectrometer. The synthesis and characterization of the osmium complexes was performed in the laboratory of Henry Taube at Stanford University. We also thank Henry Taube for his advice and encouragement. The research program of M.J.W. is supported in part by the Office of Naval Research and the Air Force Office of Scientific Research, and of H.T. by the NSF (Grant CHE 79-08633) and NIH (Grant GM 13638-17). P.A.L. acknowledges a CSIRO Postdoctoral Fellowship, and M.J.W. a Sloan Foundation Fellowship.

References and Notes

(1) (a) Purdue University; (b) Graduate research assistant, Michigan State University, 1977-81; (c) Stanford University.

(2) For reviews, see (a) Van Duyne, R. P., in "Chemical and Biochemical Applications of Lasers", Vol. 4, Moore, C. B.; Ed, Academic Press, N.Y., 1979, Chapter 5; (b) Furtak, T. E.; Reyes, J.; Surface Science, 1980, 93, 382; (c) Burke, R. L.; Lombardi, J. R.; Sanchez, L. A.; Adv. Chem. Ser., 1982, 201, 69; (d) Chang, R. K.; Laube, B. L.; CRC Crit. Rev. Solid State Mat. Sci., in press; (e) Otto, A. in "Light Scattering in Solids", M. Cardona, G. Guntherodt (eds), Springer, Berlin, 1984.

(3) (a) Weaver, M. J.; Barz, F.; Gordon II, J. G.; Philpott, M. R.; Surface Science, 1983, 125, 409; (b) Hupp, J. T.; Larkin, D.; Weaver, M. J.; Surface Science, 1983, 125, 429; (c) Weaver, M. J.; Hupp, J. T.; Barz, F.; Gordon II, J. G.; Philpott, M. R.; J. Electroanal. Chem., in press.

(4) (a) Barz, F.; Gordon II, J. G.; Philpott, M. R.; Weaver, M. J.; Chem. Phys. Lett., 1982, 91, 291; (b) Philpott, M. R.; Barz, F.; Gordon II, J. G.; Weaver, M. J.; J. Electroanal. Chem., 1983, 150, 399; (c) Barz, F.; Gordon II, J. G.; Philpott, M. R.; Weaver, M. J.; Chem. Phys. Lett., 1983, 94, 168.

(5) (a) Farquharson, S.; Weaver, M. J.; Lay, P. A.; Magnuson, R. H.; Taube, H.; J. Am. Chem. Soc. 1983, 105, 3350; (b) Taddayoni, M. A.; Farquharson, S.; Weaver, M. J.; J. Chem. Phys., in press; (c) Taddayoni, M. A.; Farquharson, S.; Li, T. T-T.; Weaver, M. J.; submitted to J. Phys. Chem.

(6) Guyer, K. L.; Ph.D. dissertation, Michigan State University, 1981.

(7) (a) Lim, H. S.; Barclay, D. J.; Anson, F. C.; Inorg. Chem., 1972, 11, 1460; (b) Lay, P. A.; unpublished results; (c) Sen, J.; Taube, H.; Acta Chem. Scand. 1979, A33, 125.

(8) For example, see Haim, A.; Prog. Inorg. Chem. 1983, 30, 273.

(9) Farquharson, S.; Lay, P. A.; Weaver, M. J.; submitted to Spectrochim. Acta.

(10) (a) Ford, P.; Rudd, De F. P.; Gaunder, R.; Taube, H.; J. Am. Chem. Soc., 1967, 90, 1187; (b) Lay, P. A.; Magnuson, R. H.; Sen, J.; Taube, H.; J. Am. Chem. Soc., 1982, 104, 7658; (c) Magnuson, R. H.; Lay, P. A.; Taube, H.; J. Am. Chem. Soc. 1983, 105, 2507.

(11) (a) Lay, P. A.; Magnuson, R. H.; Taube, H.; to be published; (b) Rudd, D. P.; Taube, H.; Inorg. Chem., 1971, 10, 1543.

(12) Bard, A. J.; Faulkner, L. R.; "Electrochemical Methods," Wiley, New York, N.Y., 1980, p. 522.

(13) Lord, R. C.; Marton, A. L.; Miller, F. A.; Spectrochim. Acta, 1957, 9, 113.

(14) Jeanmaire, D. L.; Van Duyne, R. P.; J. Electroanal. Chem., 1977, 84, 1.

(15) Dornhaus, R.; Long, M. B.; Benner, R. E.; Chang, R. K.; Surface Science, 1980, 93, 240.

(16) (a) Corrsin, L.; Fax, B. J.; Lord, R. C.; J. Chem. Phys., 1953, 21, 1170; (b) Wilmshurst, J. K.; Bernstein, H. J.; Can. J. Chem., 1957, 35, 1183.

(17) (a) Gill, N. S.; Nuttall, R. H.; Scaife, D. E.; Sharp, D. W. A.; J. Inorg. Nucl. Chem., 1961, 18, 79; (b) Clark, R. J. H.; Williams, C. S.; Inorg. Chem., 1965, 4, 350; (c) Choca, M.; Ferraro, J. R.; Nakamoto, K.; J. Chem. Soc. Dalton, 1972, 2297; (d) Akyiiz, S.; Dempster, A. B.; Morehouse, R. L.; Suzuki, S.; J. Mol. Struct., 1973, 17, 105; (e) Flint, C. D.; Matthews, A. P.; Inorg. Chem., 1975, 14, 1008.

(18) (a) Goldstein, M.; Unsworth, W. D.; Spectrochim. Acta., 1971, 27A, 1055; (b) Child, M. D., Percy, G. C.; Spect. Lett., 1977, 10, 71; (c) Child, M. D.; Foulds, A. G.; Percy, G. C.; Thorton, D. A.; J. Mol. Struct. 1981, 75, 191.

(19) (a) Senoff, C. V.; Allen, A. D.; Can. J. Chem., 1967, 45, 1337; (b) Bee, M. W.; Kettle, S. F. A.; Powell, D. B.; Spectrochim. Acta, 1974, 30A, 139; (c) Schmidt, K. H.; Muller, A.; Inorg. Chem., 1975, 14, 2183; Coord. Chem. Revs., 1976, 19, 41.

(20) For example, see Wetzel, H.; Gerischer, H.; Pettinger, B.; Chem. Phys. Lett., 1981, 78, 392.

(21) We previously attributed a weak band found at 291 cm^{-1} for $Os(NH_3)_5py$ at less negative potentials to an Os(III)-py stretching mode.[5a] However, this assignment is inconsistent with that for Os(II)-py stretching at 267 cm^{-1} in view of the decrease in the metal-pyridine bond length upon Os(III) reduction expected from the known behavior of the corresponding Ru(III)/(II) couple. See Gress, M. E.; Creutz, C.; Quisksall, C. O.; Inorg. Chem. 1981, 20, 1522.

(22) Gennett, T.; Weaver, M. J.; unpublished results.

(23) Farquharson, S.; Taddayoni, M. A.; Weaver, M. J.; in preparation.

(24) Bunding, K. A.; Bell, M. I.; Durst, R. A.; Chem. Phys. Lett. 1982, 89, 54.

(25) Buck, R. P.; Chambers, J. A.; J. Electroanal. Chem. 1982, 140, 173; Stacy, A. M.; Van Duyne, R. P.; Chem. Phys. Lett. 1983, 102, 365.

(26) Conway, B. E.; Mathieson, J. G.; Dhar, H. P.; J. Phys. Chem., 1974, 78, 1226.

(27) Hendra, P. J.; Horder, J. R.; Loader, E. J.; J. Chem. Soc. A. 1971, 1766.

(28) This follows from the greater overlap expected between the osmium 5d nonbonding orbitals and ligand π-orbitals than that expected for the less extended ruthenium 4d orbitals.

(29) Robin, M. B.; Day, P.; Adv. Inorg. Chem. Radiochem. 1967, 10, 247.

(30) Creutz, C.; Prog. Inorg. Chem. 1983, 30, 1.

Table I. Major vibrational bands for pentaammine(pyridine)osmium(III)/(II) at silver electrodes and in bulk media; influences of pyridine and ammine deuteration.

Wilson Number[a]	Symmetry Species[b]	Description[c]	N. Raman[d]	Infrared[d]		Surface-enhanced Raman[i]					
								pyridine-D_5[k]		ND_3[l]	
			Os(III)[e]	Os(III)[e]	Os(II)[g]	-150mV	-750mV	-150mV	-750mV	-150mV	-750mV
	A_1	ν_{M-py}					267s		263m		256s
	E	ν_{M-NH_3}				494w	468m	480m	460m,br	461m,br	436m
6a	A_1	δ_{ring}	654m	649w		654m	648s	623w	618m	655m	647m
11	B_2	γ_{C-H}	704m	696vs			739w			701m	698w
10b	B_2	γ_{C-H}				895w	900m		702m		898w
1	A_1	ν_{ring}	1020s	1022m	990m	1020vs	992s	978vs	955s	1019vs	989s
12	A_1	ν_{ring}		1074s	1055w	1076m	1054s	1042m,sh	1025m	1078m	1054m
9b,15	B_1	δ_{C-H}	1154vw	1157m		1151w	1151w				
9a	A_1	δ_{C-H}	1221m	1216m,br		1216m,br	1210s		896m	1220s	1210s
14	B_1	δ_{C-H}		1373s,sh		1386s	1385w	1322vs	1325m	1321s	
19b	B_1	ν_{ring}		1442vs		1441w	1430w,br			1443w	
8a	A_1	δ_{ring}	1600m,sh			1592vs,br	1593s	1552vs	1550s	1604vs,br	1593vs
	E	$\delta_{NH_3(as)}$	1613s	1608vs		1620s,br		1604vs	1600m,br	1170s	
13	A_1	ν_{C-H}				2900w,br	2910w,br		2100m,br		
7b	B_1	ν_{C-H}		2940m						2930s	2920m,br

Table II. Major vibrational bands for pentaamminepyridineruthenium(III)/(II) at silver electrodes and in bulk media; comparison with pyridine.

Wilson Number[a]	Symmetry Species[b]	Description[c]	$Ru(NH_3)_5$pyridine						pyridine	
			N. Raman[d]		infrared[d]		surface-enhanced Raman[i]		surface-enhanced Raman[j]	
			Ru(III)[f]	Ru(II)[f]	Ru(III)[f]	Ru(II)[f]	-150mV	-450mV	-150mV	-650mV
	A_1	ν_{M-py}					303vs	297vs		
	E	ν_{M-NH_3}			482m,sh	470w				
6a	A_1	δ_{ring}	646m	646m	648m	640w	654vs	655s	625w	627w
11	B_2	γ_{C-H}			703vs	693m	683s	682m		
10b	B_2	γ_{C-H}			894w				880vw,br	875vw,br
1	A_1	ν_{ring}	1023s	1011s	1017s	998s	1011s	1012s(977s)	1007vs	1006s
12	A_1	ν_{ring}			1069s	1050m	1054s	1054s(826w)	1037s	1034s
15	B_1	δ_{C-H}			1153m,sh	1150w		1144vw	1154w	1153vw
9a	A_1	δ_{C-H}	1218s	1217s	1223m		1222vs	1222s(900w)	1216m	1216m
14	B_1	δ_{C-H}			1393s	1390m				
19b	B_1	ν_{ring}			1446vs	1446s	1468m	1468m(1304w)	1445vw	
8a	A_1	δ_{C-H}	1606s	1606s		1604s	1591vs	1591s(1564s)	1597m	1597s
		δ_{NH_3}(as)			1609vs	1610s,br		(1609s)		
7b	B_1	ν_{C-H}			2951s,sh	2940s,sh				

Table III. Major vibrational bands for pentaammminepyrazineosmium(III)/(II) at silver electrodes and bulk media.

Wilson Number[a]	Symmetry Species[b]	Description[c]	N. Raman		infrared		Surface-enhanced Raman[i]			
									ND_3[j]	
			Os(III)[e]	Os(II)[e]	Os(III)[e]	Os(II)[g]	-150mV	-550mV	-150mV	-550mV
	A_1	ν_{M-pz}		287s			345vs	304vs 343s	345vs	299vs 340s
	E	ν_{M-NH_3}				450m	461w	440vw		
16b	B_{2u}	γ_{ring}					494w	496w	487w	487w
	A_g	δ_{ring}	710s	707s		700s	702s	673vs 699m	701s	670vs 700m
4	B_g	γ_{C-H}					736m	736w		739w
11	B_{2u}	γ_{ring}			816w,sh		820vw	814w	816w	807m
1	A_g	ν_{ring}	1021m	990m	1022m	1000s	1020s	985m	1019s	991m
12	B_{1u}	ν_{ring}		1070m	1090w	1067s	1093m	1067vs	1089m	1066vs
9a	A_g	δ_{C-H}	1236m	1240m	1251m	1232s	1232s	1223m	1230s	1224s
19b	B_{3u}	ν_{ring}			1441m	1445s	1464m	1464m	1464s	1464s
8a	A_g	ν_{ring}	1603m	1601s		1608s,sh	1602s	1590m	1600s	1594s
		δ_{NH_3}(as)	1614w		1606s,br	1616s				

Table IV. Major vibrational bands for pentaamminepyrazineruthenium(III)/(II) at silver electrodes and in bulk media; comparison with pyrazine.

Wilson Number[a]	Symmetry Species[b]	Description[c]	$Ru(NH_3)_5$pyrazine				pyrazine	
			N. Raman[d]	infrared[d]	surface-enhanced Raman		surface-enhanced Raman[j]	
			Ru(II)[h]	Ru(II)[h]	-150mV	-650mV	-150mV	-650mV
	A_1	ν_{M-pz}	315m,br		325s,br	302s,br		
	E	ν_{M-NH_3}	451vs	456w	455vw			
6a	A_g	δ_{ring}	692m		687s	675s	639s	636s
4	B_{3g}	γ_{C-H}			736m	735m	699m	699m
10a	B_{1g}	γ_{C-H}		753sh,br			742m	744m
11	B_{2u}	γ_{C-H}			820m	819m	806m	812m,br
1	A_g	ν_{ring}	1019m	1013m	1019s	1016s	1020s	1021s
12	B_{1u}	ν_{ring}	1076m,br		1077s	1056m,sh 1074m	1088m	
9a	A_g	δ_{C-H}	1229s	1221s	1227vs	1223s	1225s	1225s
19b	B_{3u}	ν_{ring}		1467m	1472m	1471m	1464w	1467w
19a	B_{1u}	ν_{ring}		1480m			1479w	1479w
8a	A_g	ν_{ring}	1601s	1579s	1593vs	1591s	1590vs	1588vs
		δ_{NH_3}(as)		1620s,br				

Notes to Tables I-IV

Frequencies listed are typically accurate to within 2-3 cm^{-1}.
Explanation of symbols: w = weak, m = medium, s = strong, vs = very strong, br = broad, sh = shoulder

[a]As assigned for benzene: see ref. 13.

[b]Assuming C_{2v} symmetry for pyridine or pyrazine; C_{4v} symmetry for metal-nitrogen modes.

[c]Vibrational assignments; see text and ref. 9 for details. Symbols: ν, stretching mode; δ, in-plane bending mode; γ, out-of-plane bending mode.

[d]Bulk Raman and Infrared spectra recorded as mixture of Cl^-, ClO_4^-, I^-, or PF_6^- salt to KBr or CsI in solid pellet.

[e]chloride salt

[f]perchlorate salt

[g]iodide salt

[h]hexafluorophosphate salt

[i]SER spectra obtained using ca. 0.1 - 1 m<u>M</u> complex at roughened silver electrode in either 0.1 <u>M</u> NaBr or 0.1 <u>M</u> NaCl (see text and figure captions for details). For pyridine complexes, electrolyte also contained 0.1 <u>M</u> HCl to suppress hydrolysis. Potentials quoted versus saturated calomel electrodes (sce).

[j]Obtained using 0.01 <u>M</u> pyridine or pyrazine in 0.1 <u>M</u> NaCl

[k]SER spectra for complex prepared with pentadeuterated pyridine.

[l]SER spectra for complex containing deuterated ammine ligands; prepared by dissolving complex in neutral D_2O.

Figure Captions

Figure 1

A. Cathodic-anodic cyclic voltammogram for adsorbed $Os(NH_3)_5py^{III/II}$ redox couple at roughened silver-aqueous interface in 0.1 M NaCl + 0.1 M HCl. Electrode (apparent area = 0.125 cm^2) roughened by means of an oxidation-reduction cycle in this supporting electrolyte; (roughness factor ca. 1.8 on basis of capacitance measurements[3b]). Bulk $Os^{III}(NH_3)_5py$ concentration = 50 μM; sweep rate = 100 V sec^{-1}.

B. Plots of relative surface concentrations for adsorbed $Os^{III}(NH_3)_5py$ and $Os^{II}(NH_3)_5py$ against electrode potential (solid curves), and relative peak intensities of the 1020 cm^{-1} and 992 cm^{-1} SERS vibrational modes (dashed curves) plotted against electrode potential on the same scale. Experimental conditions as for Fig. 1A. Solid lines were obtained by integrating the cyclic voltammogram in Fig. 1A as outlined in the text. Both the adsorbate surface concentrations and the SERS intensities for Os(III) and Os(II) are those relative to the values at -150 and -800 mV vs. sce (see text). SER spectra obtained using 647.1 nm irradiation.

Figure 2

A. Cathodic-anodic cyclic voltammogram for adsorbed $Os(NH_3)_5pz^{III/II}$ redox couple at silver-aqueous interface. Conditions as in Fig. 1A, except bulk Os(III) concentration = 100 μM, supporting electrolyte pH 9, sweep rate = 20 V sec^{-1}.

B. Plots of relative surface concentrations for $Os^{III}(NH_3)_5pz$ and $Os^{II}(NH_3)_5pz$ against electrode potential (solid curves), and relative peak intensities of the 1093 cm^{-1} and 1067 cm^{-1} SERS vibrational modes (dashed curves) plotted against electrode potential on the same scale. Experimental conditions as for Fig. 2A. Solid lines were obtained by integrating the cyclic voltammogram in Fig. 2A. SER spectra obtained using 647.1 nm irradiation.

Figure 3

Representative SER spectra of $Os(NH_3)_5py$ as a function of electrode potential at roughened silver; solution contained 0.1 mM $Os(NH_3)_5py^{3+}$ in 0.1 M NaBr and 0.1 M HCl. Spectral conditions: 514.5 nm excitation, 100 mW incident power, scan speed 1 cm^{-1} sec^{-1}, time constant 1 sec, resolution 4 cm^{-1}. Spectra obtained at successively more negative potentials following surface roughening by means of an oxidation-reduction cycle (see text).

Figure 4

Representative SER spectra of $Ru(NH_3)_5py$ as a function of electrode potential. Conditions as in Fig. 3, except intensity scales differed from Fig. 2A by factors indicated.

Figure 5

A. Solution Raman spectrum of $Os^{III}(NH_3)_5pz$ (lower trace) and of $Os^{II}(NH_3)_5pz$ (upper trace, x 0.5). Sample concentration = 2.5 mM. Conditions as in Fig. 3, except incident laser power was 400 mW.

B -D. Representative SER spectra of $Os(NH_3)_5pz$ as a function of electrode potential. Conditions as in Fig. 3, except supporting electrolyte was 0.1 M NaCl and intensity scales differed from Fig. 2A by factors indicated.

Figure 6

Representative SER spectra of $Ru(NH_3)_5pz$ as a function of electrode potential. Conditions as in Fig. 3, except supporting electrolyte was 0.1 M NaCl + 10^{-4} M HCl and intensity scales differed from Fig. 2A by factors indicated.

Figure 7

Representative SER spectra of $Os(NH_3)_5bpy$ as a function of electrode potential. Conditions as noted in footnote to Fig. 6.